Inelastic-Scattering Studies with Polarized Protons*

C. GLASHAUSSER,† R. DE SWINIARSKI,† AND J. THIRION
Service de Physique Nucléaire à Moyenne Energie, Centre d'Etudes Nucléaires de Saclay, Saclay, France

AND

A. D. HILL
Nuclear Physics Laboratory, Oxford, England

(Received 9 August 1967)

The inelastic scattering of 18.6-MeV polarized protons has been studied for the following nuclei: ^{48}Ti, ^{50}Ti, ^{52}Cr, ^{54}Fe, ^{56}Fe, ^{58}Ni, ^{62}Ni, ^{64}Ni, and ^{63}Cu. The targets ^{52}Cr, ^{60}Ni, and ^{62}Ni have been investigated at 16.5 MeV. The measured asymmetries for strong $l=2$ transitions tend to fall into two categories, distinguished by the magnitude of the asymmetries at 30° and 90°. Of those $l=2$ transitions studied, only those to the first 2^+ state of the 28-neutron nuclei seem to show large asymmetries at these angles. Strong $l=3$ and $l=4$ transitions also reveal several interesting variations. When the entire optical potential is deformed, coupled-channels and distorted-wave Born-approximation calculations predict the "small" $l=2$ asymmetries reasonably well, but the fits to the large asymmetries are unsatisfactory. Phenomenological calculations in the spirit of the microscopic model indicate that the predicted asymmetry is sensitive to the form factor. No important differences between $S=0$ and $S=1$ predictions were found. Simple calculations with form factors arising from single-particle transitions predict asymmetries which closely resemble those predicted with a real collective-model form factor.

I. INTRODUCTION

ANALYSES of the scattering of medium-energy projectiles in terms of the distorted-wave Born approximation[1] (DWBA) with collective-model form factors have been numerous and often satisfactory.[2–6] At least for the forward angles, this method usually gives a good account of the experimental differential cross sections for transitions to strongly excited 2^+ and 3^- states in medium and heavy nuclei; in some cases this success extends also to weaker states for which the model was not designed. The deformation or strength parameters β derived from these studies are normally consistent with those obtained in other types of experiments. The information drawn from such a macroscopic analysis is, however, essentially limited to this one parameter; moreover, such a simple model cannot explain, e.g., large differences in the experimental angular distributions for transitions with the same angular-momentum transfer in neighboring nuclei. Thus inelastic scattering has also been considered in terms of a microscopic model[7,8] of the interaction between the projectile and the target nucleons. Several recent attempts[9–12] have been made to give the theory of scattering from medium and heavy nuclei this more pleasing and potentially more fruitful basis. These studies show results which are promising but which at this time are often inferior to those of the collective model, even for weaker states.

Measurements with polarized projectiles should provide a sensitive test of these reaction models; at the very least, such experiments should help determine whether the spin-dependent forces are being treated correctly. The DWBA has had difficulty in explaining polarization measurements[13–15] and J dependence in stripping reactions[16]; moreover, the distorted-wave impulse approximation has not always been successful in fitting inelastic-scattering polarization data at high energies.[17,18] It is then interesting to discover if these difficulties persist in the interpretation of polarization in inelastic scattering at medium energies. The relevant experiments are, however, rare, since it is only recently that the requirements of a relatively intense source of

* Results of this work were submitted by one of us (R. de S.) in partial fulfillment of the requirement for a Ph.D. degree (University of Orsay).

† Present address: Lawrence Radiation Laboratory, Berkeley, California.

[1] G. R. Satchler, Nucl. Phys. **55**, 1 (1964).

[2] S. Hayakawa and S. Yoshida, Progr. Theoret. Phys. (Kyoto) **14**, 1 (1955).

[3] E. Rost and N. Austern, Phys. Rev. **120**, 1375 (1960).

[4] H. O. Funsten, N. R. Roberson, and E. Rost, Phys. Rev. **134**, B117 (1964).

[5] W. S. Gray, R. A. Kenefick, and J. J. Kraushaar, Nucl. Phys. **67**, 565 (1965).

[6] S. F. Eccles, H. F. Lutz, and V. A. Madsen, Phys. Rev. **141**, 3 (1966); **141**, 1067 (1966).

[7] N. Austern, H. Mc Manus, and S. T. Butler, Phys. Rev. **92**, 350 (1953).

[8] C. A. Levinson and M. K. Banerjee, Ann. Phys. (N. Y.) **2**, 471 (1957); **3**, 67 (1958).

[9] N. K. Glendenning and M. Veneroni, Phys. Rev. **144**, 839 (1966).

[10] G. R. Satchler, Nucl. Phys. **77**, 481 (1966), and references therein.

[11] G. R. Satchler, Nucl. Phys. **A95**, 1 (1967).

[12] N. K. Glendenning, B. G. Harvey, D. L. Hendrie, O. N. Jarvis, and J. Mahoney, in *Proceedings of the International Conference on Nuclear Physics, Gatlinburg, Tennessee, 1966* (Academic Press Inc., New York, 1967).

[13] S. A. Hjorth, J. X. Saladin, and G. R. Satchler, Phys. Rev. **138**, B1425 (1965).

[14] N. S. Chant, P. S. Fisher, and D. K. Scott, Nucl. Phys. **A99**, 669 (1967).

[15] D. W. Miller, in *Proceedings of the Second International Symposium on Polarization Phenomena of Nucleons, Karlsruhe, 1965*, edited by P. Huber and H. Schopper (Birkhauser Verlag, Basel, 1966), p. 410.

[16] C. Glashausser and M. E. Rickey, Phys. Rev. **154**, 1033 (1967).

[17] R. M. Haybron and H. Mc Manus, Phys. Rev. **140**, B638 (1965).

[18] M. Tatischeff and M. Marty (to be published).

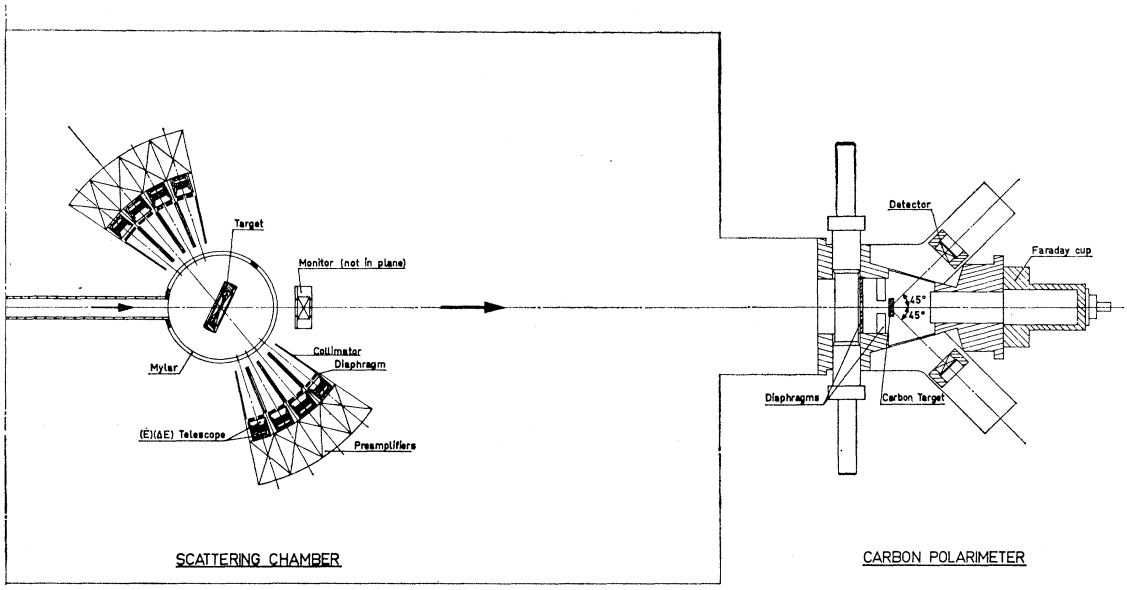

FIG. 1. Schematic diagram of detection system, drawn approximately to scale. Incident protons arrive from the left; only the small target chamber is evacuated.

polarized protons, good energy resolution, and the ability to handle data from many detectors at one time have been met. Polarization data have previously been reported for scattering to the first excited state of light nuclei[19–22] but for medium-weight nuclei, for which so many differential cross sections have been measured, polarization data did not exist at all when the present work was begun. Thus the experiments to be described here (some of which have already been the subjects of short papers),[23–25] together with those of the Oak Ridge group[26] at 40 MeV on several Fe and Ni isotopes and those of the Birmingham group[27] at 30 MeV on ^{54}Fe, constitute the first systematic analysis of this type.

In the present experiment, we measured the asymmetry in the inelastic scattering of 18.6-MeV polarized protons from targets of ^{48}Ti, ^{50}Ti, ^{52}Cr, ^{54}Fe, ^{56}Fe, ^{58}Ni, ^{62}Ni, ^{64}Ni, and ^{63}Cu. The targets ^{52}Cr, ^{60}Ni, and ^{62}Ni were also studied at 16.5 MeV. After a description of the experimental methods in Sec. II, the data for the strong $l=2$, $l=3$, and $l=4$ transitions for which we have reasonable statistics are presented in Sec. III. The analysis of the data in terms of the DWBA and the coupled-channels method is given in Sec. IV. Section V includes some comments on this analysis and a summary of the results obtained.

II. EXPERIMENTAL METHOD

All data were obtained at the Saclay sector-focused cyclotron. The polarized ion source for this machine has been previously described[28]; it utilizes the adiabatic-transition method in low and high magnetic fields as proposed by Abragam and Winter.[29] A maximum intensity of about 2×10^8 protons/sec in a spot about 2×6 mm on the target could be obtained with the system of injection and ionization used in these experiments. The average beam polarization was about 50%, although values up to about 70% were sometimes attained; the sign of the polarization was reversed every 0.2 sec.

The deflected beam passes through a switching magnet and an achromatic system of two 45° bending magnets to the scattering chamber shown in Fig. 1. The beam spot on the target is the image of an object slit placed just after the switching magnet; since no other slits were used, the energy spread of the beam was determined by the cyclotron itself. Two sets of four

[19] J. Lowe and D. L. Watson, Phys. Letters **23**, 261 (1966).
[20] R. M. Craig, J. C. Dore, G. W. Greenlees, J. Lowe, and D. L. Watson, Nucl. Phys. **83**, 493 (1966).
[21] E. Boschitz, Nucl. Phys. **30**, 468 (1962).
[22] E. Boschitz, R. W. Bercaw, and J. S. Vincent, Bull. Am. Phys. Soc. **9**, 439 (1964).
[23] P. Darriulat, J. M. Fowler, R. de Swiniarski, and J. Thirion, in *Proceedings of the Second International Symposium on Polarization Phenomena of Nucleons, Karlsruhe, 1965*, edited by P. Huber and H. Schopper (Birkhauser Verlag, Basel, 1966), p. 342.
[24] A. Garin, C. Glashausser, A. Papineau, R. de Swiniarski, and J. Thirion, Phys. Letters **21**, 73 (1966).
[25] C. Glashausser, A. Papineau, R. de Swiniarski, and J. Thirion, J. Phys. (Paris) (to be published).
[26] M. P. Fricke, R. M. Drisko, R. H. Bassel, E. E. Gross, B. J. Morton, and A. Zucker, Phys. Rev. Letters **16**, 746 (1966); M. P. Fricke, E. E. Gross, and A. Zucker, Phys. Rev. (to be published).
[27] D. J. Baugh, M. J. Kenny, J. Lowe, D. L. Watson, and H. Wojciechowski, Nucl. Phys. **A99**, 203 (1967).
[28] R. Beurtey, thesis, University of Paris, Report No. 2366 (unpublished). R. Beurtey, in *Proceedings of the Second International Symposium on Polarization Phenomena of Nucleons, Karlsruhe, 1965*, edited by P. Huber and H. Schopper (Birkhauser Verlag, Basel, 1966), p. 33.
[29] A. Abragam and J. M. Winter, Phys. Rev. Letters **1**, 375 (1958); A. Abragam and J. M. Winter, Compt. Rend. **255**, 1099 (1962).

detectors, each 11° apart, were mounted on movable arms at the left and right sides of the target chamber so that forward- and backward-angle data were taken at the same time. Note that because of the rapid reversal of the sign of the polarization it was not necessary to repeat the same angle on both sides of the beam line. Target and detector positions were known to about ±0.5°; the angular resolution, including the width of the beam, was ±2.4°.

Lithium-drifted detectors (26×10×2.5 mm³) made in this laboratory detected the scattered protons. All detectors were cooled to about −20°C by air passed through liquid nitrogen. The over-all energy resolution achieved with this system varied between 100 and 150 keV, of which about 50 keV could be attributed to beam spread and the remainder to the detectors.

Standard electronics, generally designed in this laboratory, shaped the pulses for an Intertechnique 4096-channel pulse-height analyzer. A separate preamplifier and gated amplifier were used for each of the eight detectors; the outputs were mixed and fed into one biased amplifier. The gate pulse for each amplifier came from a discriminator placed after its preamplifier, so that the noise of all eight detectors was not added. This same gate pulse served also as a routing pulse for the memory unit. A digital pulse corresponding to the two spin states of the beam was also fed to the memory, so that 16 spectra of 256 channels each were recorded at the same time. Dead time was negligible. Data were read out of the analyzer on paper tape and analyzed by hand.

Two detectors placed at 40° above and below the beam served as beam-intensity monitors. The polarization of the beam was continuously measured with a carbon polarimeter located at 60 cm from the target as shown in Fig. 1. It is essentially a copy of the Harwell polarimeter,[30] whose absolute efficiency has been measured in a triple-scattering experiment. The polarization in elastic scattering from carbon at 16.5 and 19 MeV measured with our polarimeter agrees well with the results of Boschitz[21]; further, another polarimeter, made here from the same drawings as our polarimeter, reproduces the known polarization in elastic scattering of protons from ^{4}He at various energies between 20 and 25 MeV. We thus put a probable error of ±5% on the absolute values of our measured polarization. The polarimeter consists of two detectors symmetrically placed at 45° on each side of the beam. The counting rate in the two detectors should be exactly the same if the beam is well centered and if the intensity and polarization in the two spin states are the same. In practice, the difference in beam polarization measured by the two detectors never exceeded ±2%.

Targets were obtained from Oak Ridge National Laboratory and ranged in thickness from 1–3 mg/cm². With the exception of the ^{50}Ti target which contained only 70% ^{50}Ti, all were enriched to at least 98%.

III. RESULTS

Data were obtained at 5.5° intervals from 30°–150° for most of the nuclei. The succeeding figures show ϵ, the asymmetry normalized to 100% beam polarization, as a function of the laboratory scattering angle. The parameter ϵ is thus defined as

$$\epsilon=\frac{1}{P_b}\left(\frac{N_+-N_-}{N_++N_-}\right),$$

where P_b is the measured polarization of the beam and N_+ and N_- are the counts in a peak for the spin-up and spin-down states of the proton beam, respectively. The Basel sign convention[31] is used. The errors shown in the figures are relative; the additional error of ±5% in the absolute scale is not included. Uncertainties in background polarization and in contributions from partially resolved peaks are included in the error estimates.

Several features of the $l=2$ curves illustrated in Figs. 2 and 3 are noteworthy. First, there is a striking difference in the asymmetries for the two 2^+ states seen in ^{54}Fe. Whereas the 1.41-MeV state reveals large asymmetries at 30°, 90°, and 140°, the 2.96-MeV level gives large asymmetries only at the backward angles. The strong polarization of the first excited state in ^{54}Fe is well reflected in the behavior of the curve for the 1.43-MeV first excited state of ^{52}Cr. Although the statistics for the ^{52}Cr data are not as good, data have been taken at two energies; they agree very well with the ^{54}Fe data at 30°, though somewhat less well around 90°. On the other hand, the small asymmetries of the 2.96-MeV level in ^{54}Fe match very closely the data for the 0.845-MeV first excited state in ^{56}Fe, and these two curves are quite similar to the curves for the first excited state in all the Ni isotopes and to the two curves for Cu. The asymmetries for Ni tend to be slightly more negative in the forward direction and show a deeper minimum at about 110°. However, if we disregard the latter differences, the data thus far discussed are neatly divided into two categories, the one with "large" asymmetries like the first 2^+ state in ^{54}Fe and the other with "small" asymmetries like ^{56}Fe. Since the only two members of the large asymmetry group, ^{52}Cr and ^{54}Fe. both have 28 neutrons, it is then tempting to assign the first 2^+ state of ^{50}Ti to this group also. If the 28-neutron criterion is correct, the 0.99-MeV state in ^{48}Ti must then be put in the small asymmetry group. The 3.8-MeV state in ^{52}Cr would then be put in the small group in analogy with the 2.96-MeV level of ^{54}Fe. The error bars on these Ti and Cr data are, however, quite large. Even so, the

[30] R. M. Craig, J. C. Dore, G. W. Greenlees, J. S. Lilley, J. Lowe, and P. C. Rowe, Nucl. Instr. Methods **30**, 269 (1964).

[31] *Proceedings of the International Symposium on Polarization Phenomena of Nucleons, Basel, 1960*, edited by P. Huber and K. P. Meyer (Birkhauser Verlag, Basel, 1961).

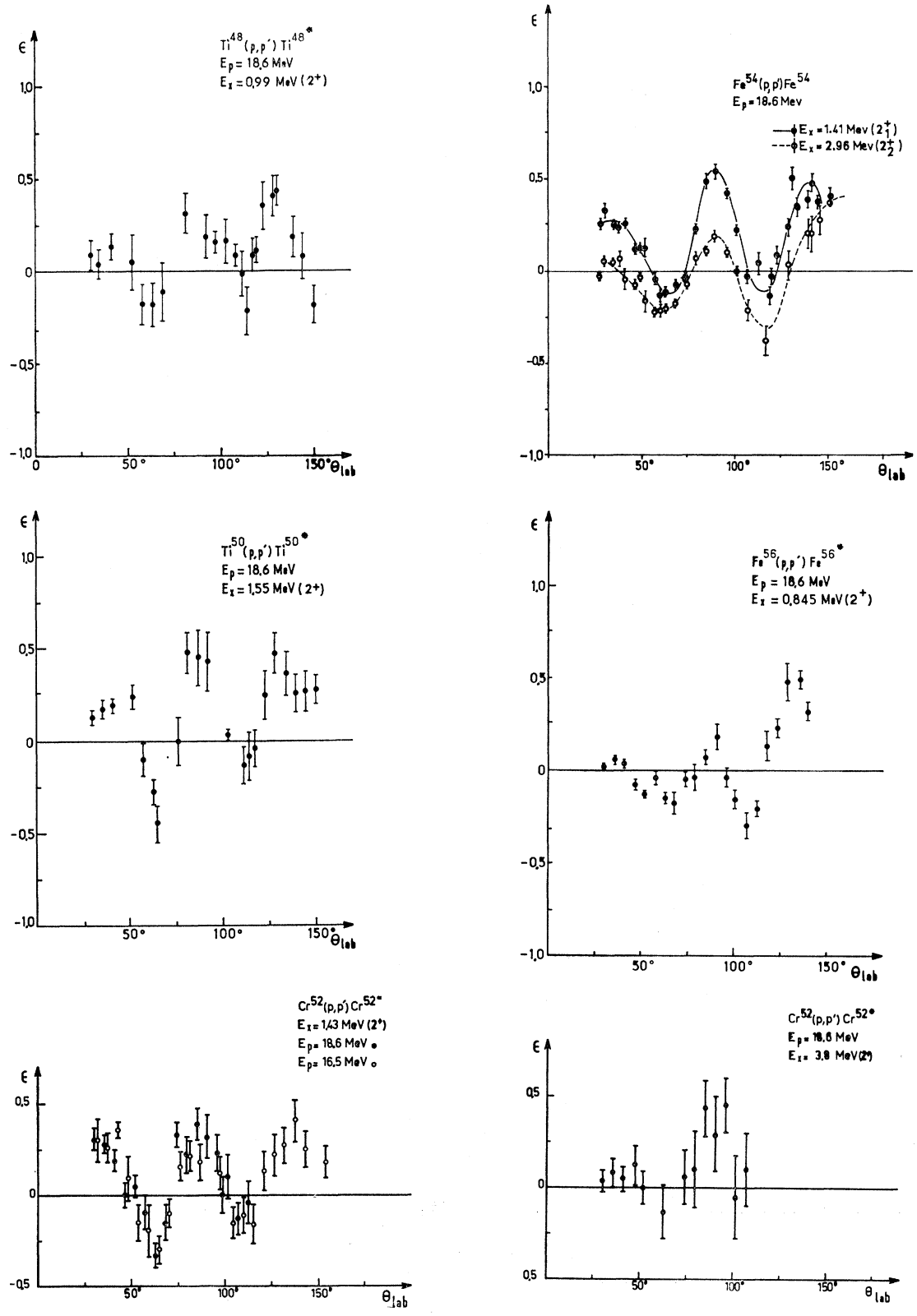

FIG. 2. The measured asymmetry ϵ, normalized to 100% beam polarization, as a function of laboratory scattering angle for $l=2$ transitions. The error bars are relative and include background subtraction. The lines drawn for ^{54}Fe are visual guides.

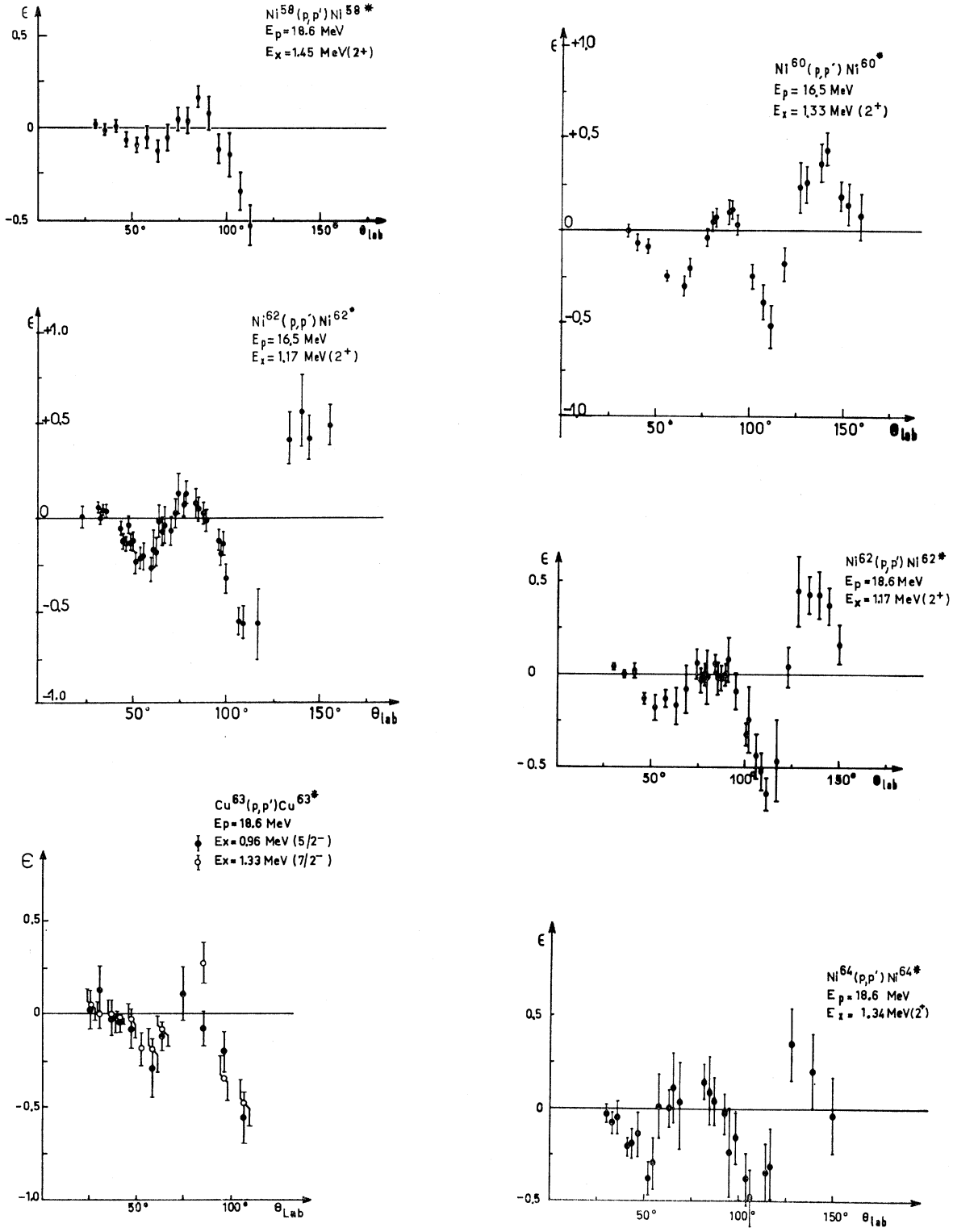

FIG. 3. The measured asymmetry ϵ as a function of laboratory scattering angle for $l=2$ transitions in Ni and Cu isotopes.

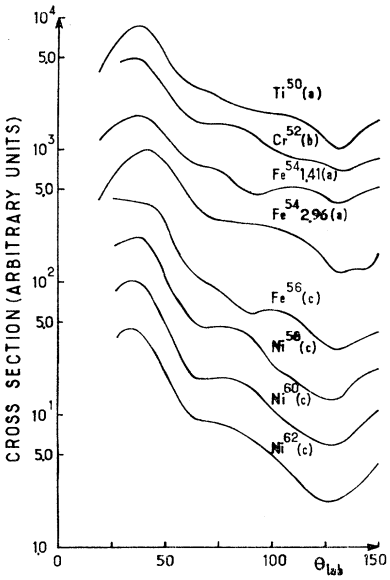

FIG. 4. Differential cross sections as a function of laboratory scattering angle for the first 2^+ states in several nuclei. The 2^+ state at 2.96 MeV in ^{54}Fe is also shown. The references are the following: (a), Ref. 5, (b), Ref. 33, (c), Ref. 6.

data do not seem to support such a convenient assignment.

The data from related experiments do not give definite support to such a division. The asymmetry corresponding to the 1.41-MeV level of ^{54}Fe has been measured at 30 MeV[27]; the data appear quite similar both in magnitude and in general shape to the 18.6-MeV curve reported here. At 40 MeV,[26] the asymmetry has increased greatly in magnitude at angles larger than 60°, and the shape of the curve has changed considerably. Within the error bars, which are generally larger than those of Fig. 2, the four asymmetries reported by the Oak Ridge group for the 1.41- and 2.96-MeV states in ^{54}Fe and the first excited states in ^{60}Ni and ^{62}Ni all look the same. In $(p,p'\gamma)$ experiments at 11 MeV, Ballini *et al.*[32] have found that the spin-flip probability in the transition to the first 2^+ states of ^{52}Cr and ^{54}Fe shows a distribution as a function of scattering angle which is different from the pattern established in the Ni and Zn isotopes, but the ^{52}Cr and ^{54}Fe distributions are also different from each other. If one looks at the inelastic-scattering cross sections themselves at about 18 MeV, he notes that here also there are variations in shape among the $l=2$ curves. The angular distributions of Fig. 4, taken from various sources,[5,6,33] show clear differences at large angles; the ratio of the back-angle cross section to the maximum cross section is much smaller for nuclei with more than 28 neutrons than for $f_{7/2}$ shell nuclei. Even among the latter, there are small but noticeable differences at forward as well as backward angles. The four 2^+ states observed in the Ni isotopes, however, have very similar relative cross sections.

These first excited states in the Ni isotopes have long been known to be collective states[34–36]; usually they are simply described as one-phonon states in a vibrational model. The first 2^+ states in the 28-neutron isotopes ^{50}Ti, ^{52}Cr, and ^{54}Fe are considered to be dominantly $(f_{7/2})^{\pm n}$ proton configurations,[4,11,37] though the admixtures of other configurations are not well known. As a means at least of parameterizing the data, analyses of inelastic scattering cross sections to these states have also made use of the vibrational model and derived a deformation parameter β_l. The values obtained in this way for β from several recent experiments are shown in Table I. It is clear that the 2^+ states in ^{56}Fe and in the Ni isotopes are the most "collective." Little is known about the higher 2^+ states in ^{52}Cr and ^{54}Fe, though there are indications that they arise primarily from excitation of a $p_{3/2}$ particle. Whitten,[33] e.g., has seen a strong, apparently pure $l=3$ transition to the 3.77-MeV 2^+ state in ^{52}Cr by the ^{53}Cr(p,d) reaction at 17.5 MeV, while the strong transition to the first 2^+ state proceeds by $l=1$; he is thus led to suggest that the first state is a good closed $f_{7/2}$ shell neutron configuration while the neutron configuration of the higher state is mostly $(f_{7/2}^{-1}p_{3/2})$. Concerning the second 2^+ state at 2.96 MeV in ^{54}Fe, it is to be noted only that this state and the first excited state cannot both arise from a pure $(f_{7/2}^{-2})$ proton configuration, and also that the cross section is too large for a two-phonon contribution to be dominant. The low-lying states of ^{63}Cu have been

TABLE I. Deformation parameter β determined from (p,p') and (α,α') experiments.

		(p,p') (a)	(b)	(c)	(α,α') (d)
^{48}Ti	2_1^+		0.21		0.19
^{50}Ti	2_1^+		0.15		0.13
^{52}Cr	2_1^+		0.17		0.13
	2_3^+		0.11		0.14
^{54}Fe	2_1^+	0.17	0.14		0.14
	2_2^+	0.15	0.13		0.12
^{56}Fe	2_1^+	0.31			0.27
	3_1^-	0.22			0.11
^{58}Ni	2_1^+	0.24			0.31
	3^-	0.19			0.13
^{60}Ni	2_1^+	0.28			0.28
^{62}Ni	2_1^+	0.30		0.229	0.23
	3^-	0.24		0.187	0.19
^{64}Ni	2_1^+			0.200	0.20
	3^-			0.181	0.18
^{63}Cu	$\frac{5}{2}^-$			0.265	
	$\frac{7}{2}^-$			0.234	

[a] Reference 6.
[b] Reference 4.
[c] Reference 38(a).
[d] Reference 36.

[32] R. Ballini, N. Cindro, J. Delaunay, J. Fouan, M. Loret, and J. P. Passerieux, Nucl. Phys. **A97**, 561 (1967).
[33] C. Whitten, thesis, Princeton University (unpublished); Phys. Rev. **156**, 1228 (1967).
[34] B. L. Cohen and A. G. Rubin, Phys. Rev. **111**, 1568 (1958); **113**, 579 (1959).
[35] R. Beurtey *et al.*, Compt. Rend. **252**, 1756 (1961).
[36] G. Bruge, thesis, University of Paris, 1967 (unpublished).
[37] J. D. MacCullen, B. F. Bayman, and L. Zamick, Phys. Rev. **134**, 515 (1964).

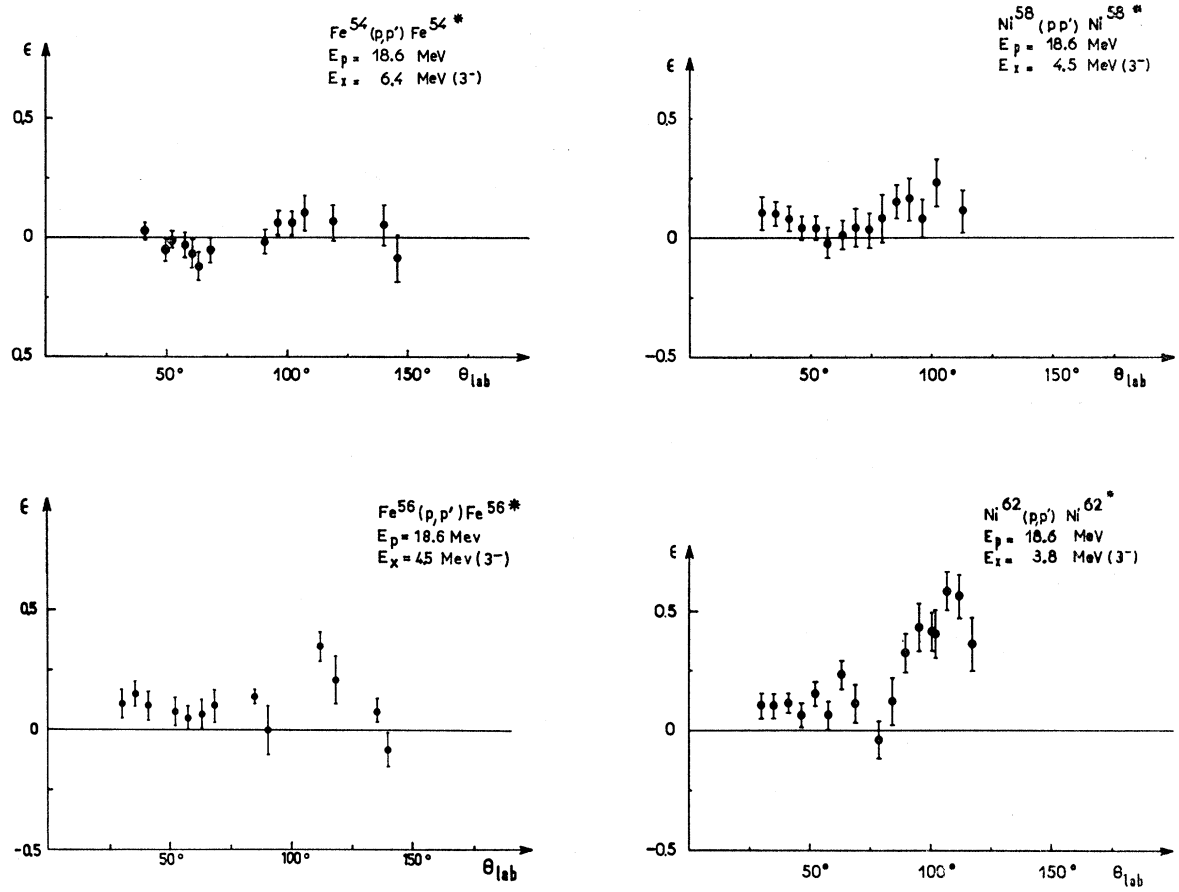

FIG. 5. The measured asymmetry ϵ as a function of laboratory scattering angle for $l=3$ transitions.

the subject of many experiments[38] and several calculations.[39] While inelastic-scattering experiments give general but not complete agreement with a weak-coupling model for these states, stripping and pickup experiments indicate that the single-particle aspects are dominant. The puzzle is not yet solved, but the more sophisticated calculations can at least partially explain both single-particle and collective contributions.

The data for the collective 3^- states and the 4^+ states are shown in Figs. 5 and 6. The 3^- data are not extensive enough, and the error bars are not small enough to permit significant conclusions. Here again, however, variations in the shape of the curves, especially around 100°, are apparent, though it is possible that a polarized background contribution from nearby states could cause some of these differences. The two 4^+ states that are shown in Fig. 6 give remarkably different asymmetries. The 2.56-MeV state in ^{54}Fe has been consistently assigned 4^+ in (p,p')[4,5,40] and (α,α')[35,36] measurements; it obeys the Blair phase rule for one-phonon transitions at 44 MeV in (α,α'). However, in addition to this level, other states at 2.534 and 2.540 MeV have been seen in the high resolution inelastic-scattering work of the MIT group,[41] and they could be contributing to the excitation. The 4^+ state in ^{58}Ni, however, seems quite clearly resolved from other states.[42] This level appears as a pure two-phonon transition in (α,α') work at 44 MeV,[36] but large variations in the angular distribution as a function of α energy indicate that one-phonon contributions are also important.[43]

IV. ANALYSIS

A. Optical Potential

The optical-model parameters used in the DWBA analyses which follow were determined from an analysis

[38] (a) A. L. McCarthy and G. M. Crawley, Phys. Rev. **150**, 935 (1966); (b) see also A. G. Blair, *ibid.* **140**, B648 (1965); G. Bruge, J. C. Faivre, M. Barloutaud, H. Faraggi, and J. Saudinos, Phys. Letters **7**, 203 (1963); F. G. Perey, R. J. Silva, and G. R. Satchler, *ibid.* **4**, 25 (1963).

[39] W. Beres, Phys. Letters **16**, 65 (1965); U. W. Thankappan and W. W. True, Phys. Rev. **137**, B793 (1965).

[40] M. F. Thomas, A. R. Poletti, and M. A. Grace, Nucl. Phys. **78**, 561 (1966).

[41] A. Sperduto and W. W. Buechner, Phys. Rev. **134**, B142 (1964).

[42] E. R. Cosman, Ch. Paris, A. Sperduto, and H. A. Enge, Phys. Rev. **142**, 673 (1966).

[43] J. Meriwether, B. G. Harvey, A. Bussière de Nercy, and J. Mahoney, Nucl. Phys. **72**, 97 (1965).

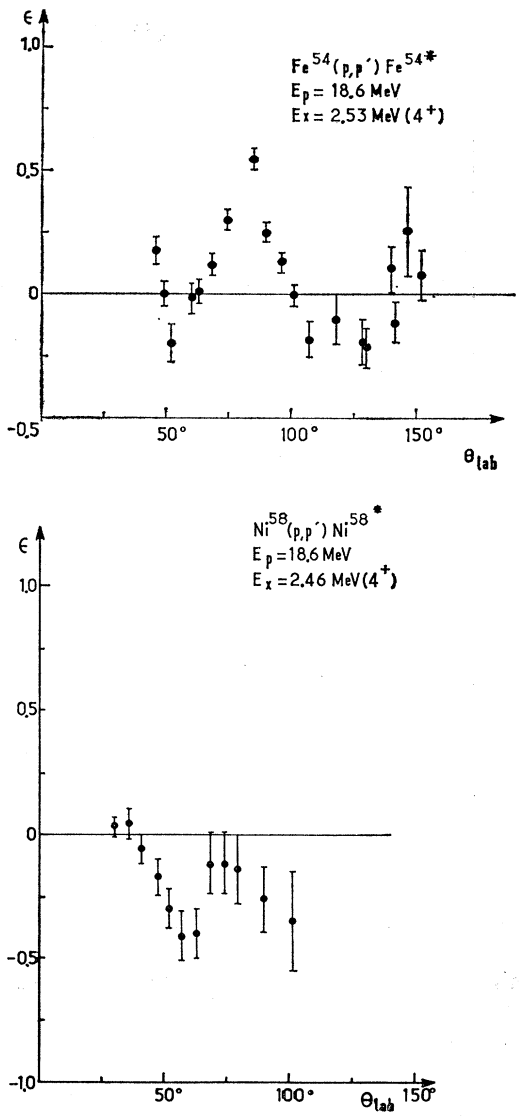

FIG. 6. The measured asymmetry ϵ as a function of laboratory scattering angle for $l=4$ transitions in ^{54}Fe and ^{58}Ni. Other unresolved levels may be contributing to the ^{54}Fe distribution.

of the elastic polarization data taken concurrently with the inelastic data; the elastic cross sections were taken from various sources. The optical potential has the standard form

$$U(r)=-V_s(r,r_s,a_s)+i[W_s f(r,r_I,a_I) -4a_I W_D(d/dr)f(r,r_I,a_I)]+(\hbar/m_\pi c)^2 \times(V_{so}+iW_{so})\mathbf{l}\cdot\boldsymbol{\sigma}r^{-1}(d/dr)f(r,r_{so},a_{so}), \quad (1)$$

to which is added the Coulomb potential of a uniformly charged sphere. The functions $f(r,r_i,a_i)$ are of the Woods-Saxon form.

Previous analyses of these data[44] with the central geometrical parameters fixed at values determined by

[44] P. Kossanyi-Demay, R. de Swiniarski, and C. Glashausser, Nucl. Phys. **A94**, 513 (1967).

TABLE II. Optical-parameter set A. The geometrical parameters except r_{so} were kept fixed at the following values: $r_c=1.25$ F, $r_s=r_I=1.25$ F, $a_s=0.65$ F, and $a_I=a_{so}=0.47$ F. The parameter W_s was set equal to zero; the others, V_s, W_D, V_{so}, and r_{so} varied simultaneously. Measurements for the first set of nuclei were made at 18.6 MeV; for the second set, the energy was 16.5 MeV.

A	V_s (MeV)	W_D (MeV)	V_{so} (MeV)	r_{so} (F)	σ_R (mb)	χ^2
48	50.5	11.0	5.4	1.09	995	314
50	50.6	11.6	6.4	1.21	1017	353
52	48.9	10.7	7.15	1.15	988	79
54	50.5	11.60	5.2	1.16	1009	2050
56	50.2	12.2	7.30	1.17	1016	645
58	48.5	9.3	7.2	1.17	953	190
60	51.0	11.0	6.15	1.09	1023	89
62	51.0	11.4	6.25	1.17	1045	290
63	50.2	10.1	4.7	1.11	1019	175
64	50.3	11.9	5.6	1.11	1069	328
52	51.5	9.7	4.6	1.07	1142	963
60	49.15	11.3	5.4	1.12	1000	1424
62	49.4	11.9	6.2	1.12	1032	1401

Perey[45] give the parameters in set A (Table II). It is now clear that fits which are equally good and sometimes better can be obtained by choosing radii for the real term which are smaller than the radii for the imaginary term; these parameters, which correspond to those obtained by several authors at 30[46] and 40 MeV,[47] are given in set B (Table III). It is interesting to note that r_{so} remains about 10% smaller than r_s.[48]

Since, as will be shown later, the inelastic polarization is quite sensitive to an imaginary spin-orbit term in the optical potential, we have also tried to obtain fits to the elastic data with this term included. As shown in Table IV, when W_{so} is arbitrarily fixed at certain values and the geometrical parameters are set equal to those of the real spin-orbit term, the value of χ^2 increases

TABLE III. Optical-parameter set B. The geometrical parameters except r_{so} were kept fixed at the following values: $r_c=1.1$ F, $r_s=1.1$ F, $r_I=1.3$ F, $a_s=0.75$ F, and $a_I=a_{so}=0.55$ F. The parameter W_S was set equal to zero; the others, V_s, W_D, V_{so}, and r_{so} varied simultaneously.

A	V_s (MeV)	W_D (MeV)	V_{so} (MeV)	r_{so} (F)	χ^2	σ_R (mb)
48	61.03	8.45	5.6	0.95	277	1021
50	60.83	8.85	5.67	1.01	358	1061
52	59.38	9.3	6.5	0.96	168	1063
54	61.44	9.8	5.94	1.04	1464	1075
56	60.96	9.01	6.35	0.97	560	1076
58	59.97	8.54	6.0	0.97	318	1058
62	62.07	9.00	7.14	0.98	430	1101
63	60.71	8.89	6.34	0.99	469	1095
64	61.20	10.59	7.0	0.94	388	1158

[45] F. G. Perey, in *Proceedings of the Second International Symposium on Polarization Phenomena of Nucleons, Karlsruhe, 1965*, edited by P. Huber and H. Schopper (Birkhauser Verlag, Basel, 1966), p. 191.

[46] G. R. Satchler, Nucl. Phys. **A92**, 273 (1967).

[47] M. P. Fricke and G. R. Satchler, Phys. Rev. **139**, B567 (1965).

[48] G. W. Greenlees, G. J. Pyle, and Y. C. Tang, Phys. Rev. Letters **17**, 33 (1966); D. W. L. Sprung and P. C. Bhargava, Phys. Rev. **156**, 1185 (1967).

TABLE IV. Optical parameters with imaginary spin-orbit term. In obtaining the values in the first half of the table, the program searched on V_s, W_D, V_{so}, and r_{so}. For the second half of the table, W_{so} was also a free parameter.

A	V_s	r_s	a_s	W_D	r_I	a_I	V_{so}	W_{so}	r_{so}	a_{so}	χ^2
54	61.18	1.1	0.75	9.93	1.3	0.55	5.95	−0.5	1.00	0.55	1890
54	61.26	1.1	0.75	10.20	1.3	0.55	6.1	−0.75	0.99	0.55	2585
54	60.87	1.1	0.75	11.77	1.3	0.55	6.5	−1	0.98	0.55	4186
54	59.21	1.1	0.75	8.57	1.35	0.55	5.66	−0.13	1.01	0.55	1525
52	58.92	1.1	0.75	7.63	1.35	0.55	5.64	−0.08	0.97	0.55	182
56	61.06	1.1	0.75	9.36	1.3	0.55	6.2	−0.5	0.93	0.55	669

rather rapidly. When W_{so} is allowed to vary, its final value is close to zero.

Finally, we have varied the shape of the spin-orbit term by allowing the exponent of r in the spin-orbit term of Eq. (1) to take on values other than -1. If V, W_D, V_{so}, and r_{so} are free, and the other parameters fixed, equally good values of χ^2 can be found for all values of the exponent between 0 and -2. Only the magnitude V_{so} of the spin-orbit potential changes significantly with the exponent; V_s, W_D, and r_{so} show negligible variation.

B. Reaction Models

The inelastic data have been analyzed in terms of the conventional DWBA, using the Oak Ridge computer code JULIE,[49] and also by the coupled-channels method, using the Oxford program.[50] These approaches are well known.[1,51] Each uses the same type of interaction matrix element or form factor which can be calculated according to a macroscopic or microscopic model of the interaction.

1. *Macroscopic Treatment*

In a standard calculation, when a vibrational model is assumed for the nuclear states, the shape of the form factor is given by the radial derivative of the optical potential. The shape is thus the same for all states in the same nucleus. To describe differential cross sections, only the central terms of the optical potential have normally been included in the calculation of the form factor. However, in order to explain their polarization data at 40 MeV, Fricke *et al.*[26] have shown that the spin-orbit term must also be deformed. Now the strict Thomas form of the spin-orbit potential includes non-radial terms arising from the gradient of the potential. These terms do not contribute to elastic scattering from a spin-zero nucleus, although they could appear in elastic scattering on a deformed nucleus with spin or in inelastic scattering on a vibrational or rotational nucleus. These terms have been neglected by Fricke *et al.* on the basis of simplicity. The fact that little difference is seen in the polarization in elastic scattering on neighboring deformed nuclei[52] indicates their effect is small, but these measurements are limited in number. However, there is no fundamental reason to assume that the strict Thomas form is the correct form of the spin-orbit potential; the fact that r_{so} does not equal r_s is already a departure from this form. If we accept the spin-orbit term of Eq. (1) as phenomenologically given, then the multipole expansion of the spin-orbit potential takes the following form:

$$V^{ls}(r,\xi)=\tfrac{1}{2}\sum_{Qq}[i^Q Y_Q{}^q(\hat{r})\mathbf{l}\cdot\mathbf{s}+\mathbf{l}\cdot\mathbf{s}i^Q Y_Q{}^q(\hat{r})]^* \times T_Q{}^{ls}(r,\xi) \quad (2)$$

and the form factors for the first- and second-order spin-orbit terms in the interaction become

$$V_{so}{}^{(1)}(r)=(\hbar/m_\pi c)^2 V_{so}(R/a^2r^2)2e^x(1+e^x)^{-3} \times\{a(1+e^x)+r(e^x-1)\}, \quad (3)$$

$$V_{so}{}^{(2)}(r)=(\hbar/m_\pi c)^2 V_{so}(a^2/a^3r^3)(1+e)^{-4} e^x\{r^2(e^{2x}-4e^x+1)+2ar(e^{2x}-1)+2a^2(1+e^x)^2\}. \quad (4)$$

In Eq. (2) $Y_Q{}^q$ and $T_Q{}^q$ are the usual spherical-tensor operators. The duplication of the $\mathbf{l}\cdot\mathbf{s}$ term within the brackets is necessary because $\mathbf{l}\cdot\mathbf{s}$ does not commute with $Y_Q(\hat{r})$. In Eq. (3), V_{so}, R_{so}, and a_{so} are the parameters of the optical model spin-orbit term and x is equal to $(r-r_{so}A^{1/3})/a$. The form of Eq. (3) is slightly different from that used by Fricke *et al.*; the term $[a(1+e^x)]$ was not included in their work. However, we shall mention some calculations with different forms for the spin-orbit term in the optical potential which indicate that the details of the distorted spin-orbit term are not important. All calculations which included the distorted spin-orbit term were made with the coupled-channels code.

2. *Microscopic Treatment*

A potentially more satisfying description of inelastic scattering considers explicitly the two-body interaction between the incoming proton and the target nucleons.

[49] We are grateful to Dr. R. Drisko for making this program available to us.
[50] A. D. Hill (to be published).
[51] T. Tamura, Rev. Mod. Phys. 37, 679 (1965).
[52] L. Rosen, in *Proceedings of the Second International Symposium on Polarization Phenomena of Nucleons, Karlsruhe, 1965*, edited by P. Huber and H. Schopper (Birkhauser Verlag, Basel, 1966), p. 264.

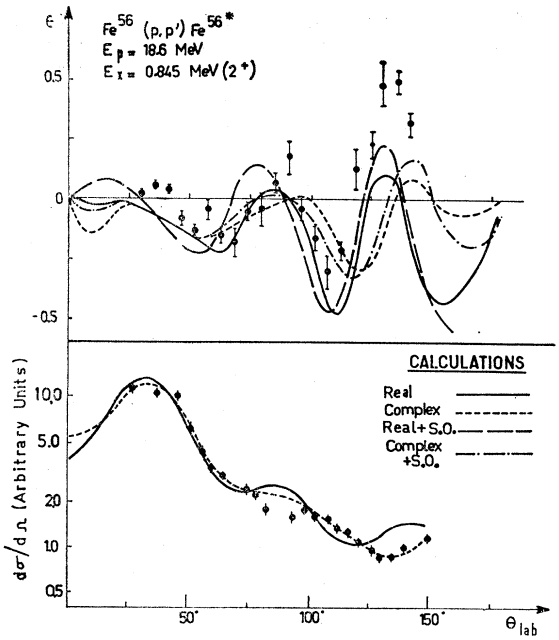

FIG. 7. Comparison of theoretical predictions with the experimental asymmetry and cross-section data for the 2^+ state in ^{56}Fe. Set-A optical parameters were used. The collective-model form factor had the same geometrical parameters as the optical potential.

The form factor in such a microscopic model assumes a wide variety of shapes, since the nuclear states can be described in terms of their shell-model configurations. The microscopic model offers more hope than the collective model of explaining the different asymmetries for for the two 2^+ states in ^{54}Fe, e.g., since the slight difference in excitation energy of the two states can produce only a negligible difference in the predicted collective-model asymmetries. In a microscopic model with a well-established interaction, one could hope to derive nuclear-structure information directly from the shapes of asymmetry and differential cross-section curves. However, a recent review of microscopic calculations by Satchler[11] indicates that the form presently chosen for the interaction is probably too simple; other types of spin dependence and probably imaginary terms must be included. As discussed below, the analysis of the present data forms part of the basis for this conclusion.

C. Calculations

Figures 7 and 8 illustrate the fact that the DWBA with a collective-model form factor can give a reasonable but certainly not perfect fit to the asymmetries of the small group. Shown here are predictions for the ^{56}Fe 0.845-MeV state when only the real central term of the optical-model potential is considered to be deformed ("REAL"), when both real and imaginary central terms are deformed ("COMPLEX"), when the real central and the spin-orbit terms are deformed ("REAL +S.O."), and when all three terms are deformed ("COMPLEX+S.O."). Parameter set A (Table I) was used for the calculation of Fig. 7, parameter set B for Fig. 8. The imaginary spin-orbit strength was zero and the deformation parameter β was kept equal for all interaction terms.

The best agreement with the asymmetry data is obtained by deforming the entire optical potential and using parameter set B. In Fig. 7, the introduction of complex and spin-orbit distortions does not make a great improvement in the fit. In fact, the two extra terms tend to act in different directions; the spin-orbit distortion increases the predicted asymmetry while the imaginary central term generally reduces it. When both are included, the prediction is similar to that with a real central term only. On the other hand, when the radius of the real and imaginary central terms in the optical potential are no longer the same, as in Fig. 8, both the imaginary and the spin-orbit interaction terms make a significant improvement in the fit. The quality of this fit is comparable with those achieved at 40 MeV,[26] but the effect of the imaginary and spin-orbit deformations is more dramatic at 40 MeV than at 18.6 MeV. The general characteristics of these predictions change very little from nucleus to nucleus, so that the fits to the 2^+ states in the Ni isotopes are slightly better in the forward angles than those shown here since the experimental points are somewhat more negative.

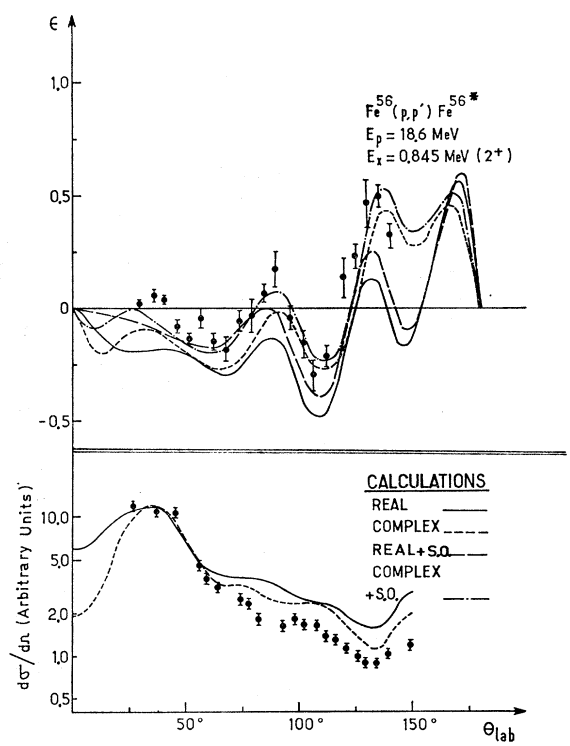

FIG. 8. Predictions of the asymmetry and differential cross section for the 2^+ state in ^{56}Fe with set-B optical parameters. The collective-model form factor also had set-B geometry.

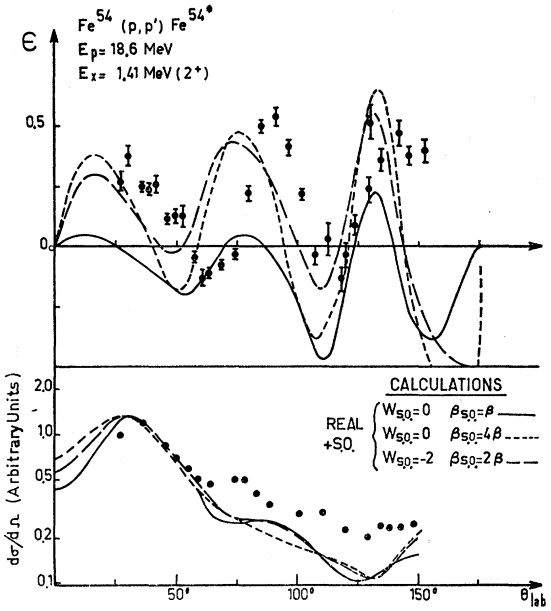

FIG. 9. Predictions of the asymmetry and differential cross section for the 1.41-MeV 2^+ state in ^{54}Fe. Set-A optical and form-factor parameters were used with the addition of an imaginary spin-orbit term (W_{so}) where noted. The amplitude of the spin-orbit deformation (β_{so}) was modified as shown. No imaginary term was included in the direct interaction.

However, such curves clearly give poor agreement with the asymmetry for the 1.41-MeV state in ^{54}Fe.

The predictions for the differential cross section for the 2^+ state in ^{56}Fe are also shown in Figs. 7 and 8. Curves calculated with a distorted spin-orbit term are not included since this term hardly affects the prediction. It is clear from these figures that the parameters which give the best fit to the polarization data do not give the best agreement with the cross sections. The curve of Fig. 7 calculated with the real interaction gives a reasonable fit to the ^{56}Fe angular distribution, and the addition of an imaginary term preserves the correct magnitude and improves the phase agreement at large angles.

On the other hand, neither cross-section prediction of Fig. 8 gives good agreement with the results, but here also the imaginary term improves the fit. To fit the differential cross section for the 1.41-MeV state of ^{54}Fe, the situation is reversed. As shown at the bottom of Fig. 9, the set-A parameters give a poor fit at large angles. Since the ratio of back-angle cross section to forward-angle cross section is larger when set-B parameters are used, the set-B predictions (not illustrated) improve the fit.

To obtain better agreement with the large asymmetries of the ^{54}Fe type, it is necessary to artificially increase the relative magnitude of the distorted spin-orbit term by a factor of 4 or to include a negative imaginary spin-orbit term in the optical potential. As shown in Fig. 9, the agreement in phase is still poor, but the magnitudes of the predicted asymmetries then agree quite well with the data. Set-A parameters were used. The predictions are not sensitive to an imaginary distorted spin-orbit term; it is the effect of W_{so} on the optical-model wave functions themselves which increases the predicted asymmetry. As mentioned above, however, the fit to the elastic scattering is lost if W_{so} is not close to zero. The optical potentials used to fit the 40-MeV elastic and inelastic scattering[26] generally included a small imaginary spin-orbit term of the order of 0.5 MeV; it was also necessary to use a β for the spin-orbit term 1.5 times larger than β for the central terms. Although a small increase in β can probably be justified in view of uncertainties in the distorted spin-orbit term, the factor of 4 needed here is unreasonable and only illustrates the failure of the model.

The asymmetry predicted for these states by the coupled-channels code was very little different from that calculated in the DWBA. Even if a coupling of the order of the ground-state, first 2^+ state coupling is introduced between the 2^+ state and, e.g., the 3^- state, the changes noted in the inelastic scattering are small.

Variations in the shape of the spin-orbit term in the optical potential as described above for the elastic scattering also do not produce important modifications in the inelastic asymmetry predictions. Even when the new spin-orbit term is distorted, the predictions are very nearly the same as standard calculations with a distorted spin-orbit term. Thus, while there is no reason *a priori* to assume the Thomas form, it works as well as any other form tried, provided, of course, that the spin-orbit radius is kept smaller than the radius of the real central term.

If we now use geometrical parameters of the collective-model form factor which are different from the optical-model parameters, rather large changes can be produced in the predicted asymmetries. Form factors

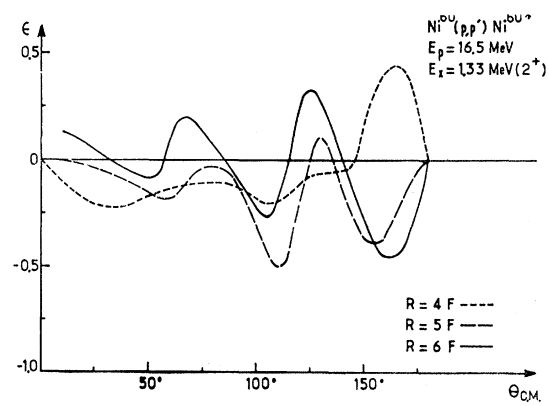

FIG. 10. The variation in DWBA predictions for the 2^+ state in ^{60}Ni when the geometry of the collective-model form factor is independent of the optical parameters. Set-A optical parameters were used in this calculation with only a real central interaction term. The radius of the form factor varied from 4–6 F as shown; the diffuseness was 0.65 F.

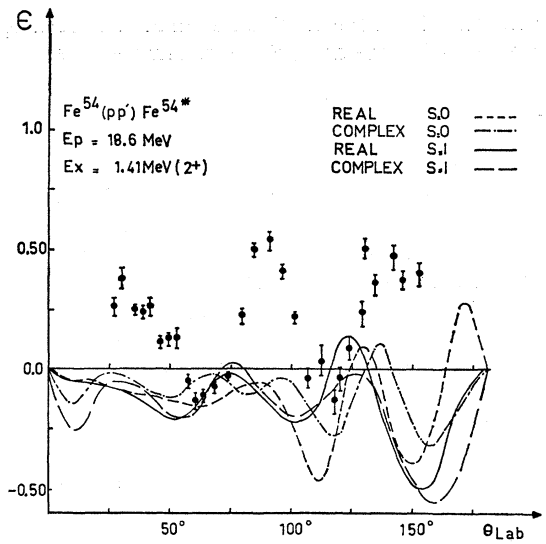

FIG. 11. Comparison of DWBA predictions when $S=0$ or $S=1$ transfer is assumed. The same collective-type form factor was used for both $S=0$ and $S=1$ calculations; set-A optical and form-factor parameters were used.

calculated for collective 2^+ states on the basis of theoretically given nuclear wave functions often are similar in general shape to collective-model form factors.[9–11] Thus these form factor variations could be considered as a phenomenological approach to a microscopic model. An example of such phenomenological calculations is shown in Fig. 10, where the radius of the real term, the only term distorted, has been varied from 4–6 F. Whereas the predicted cross section is hardly affected by such changes, the asymmetry is quite sensitive to them. Differences of this order of magnitude can also arise from reasonable variations in the diffuseness of the real term and the geometrical parameters of the imaginary term. The parameters of the distorted spin-orbit term, on the other hand, have only a small effect on the asymmetries; likewise, large variations of the form factor in the nuclear interior do not produce important changes in the predictions. A calculation with a second derivative Woods-Saxon form factor, however, can produce asymmetries much larger than those of Fig. 10, even with real coupling only.

In the same spirit, a number of calculations were performed assuming that spin transfer ($S=1$) also occurs in the interaction. Spin transfer can arise from a $\boldsymbol{\sigma}_i\cdot\boldsymbol{\sigma}_p$ interaction term in a microscopic model. The range of form factors tried covered many of those used in calculations without spin transfer. Figure 11 gives a typical example of the two types of calculations. Set-A optical parameters were used; the geometrical parameters of both $S=0$ and $S=1$ form factors were the same as the optical parameters. The predictions are not radically different. Depending on the form factor and the optical parameters, the differences are sometimes greater than those shown here, but the $S=1$ calculations have not produced an important improvement in the fit to the large asymmetries at forward angles. In some cases an $S=1$ contribution significantly improved the fit to an asymmetry of the small group, but an equally good fit can be obtained without an $S=1$ contribution by changing other parameters.

Microscopic-model calculations with shell-model wave functions for the present ^{54}Fe data have recently been

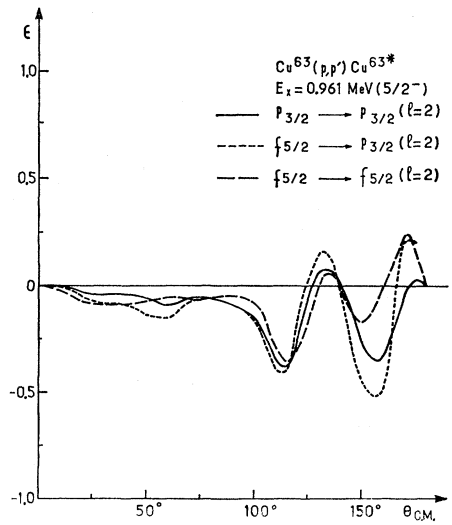

FIG. 12. Predictions of the DWBA for ^{63}Cu. The single-particle transitions are assumed in the calculation of the form factor; a real Gaussian interaction with a range of 1.85 F was used. Set-A optical parameters were employed and no spin-flip was allowed.

carried out by Satchler.[11] With an interaction of the form

$$V_{ip}(r)=-(V_0+V_1\boldsymbol{\sigma}_i\cdot\boldsymbol{\sigma}_p)f(r_{ip}), \qquad (5)$$

he was unable to find good fits for either the first or second 2^+ states. Simple $(f_{7/2}^{-2})$ or $(f_{7/2}^{-3}p_{3/2})$ configurations were assumed for the excited states, and $(f_{7/2}^{-2})$ configurations for the ground state. These form factors differed from collective-model form factors mostly in the nuclear interior, and the predicted asymmetries are similar to those of Figs. 7 and 8 with real distortions only. We have performed similar calculations for ^{63}Cu, where it is likely that more configurations enter into the excitation. The results, some of which are shown in Fig. 12 for an $S=0$ Gaussian interaction with a range of 1.85 F, again closely resemble the predictions of a collective model with a real form factor. On the other hand, using a simple Gaussian interaction in Eq. (5) and quasiparticle wave functions calculated with a surface delta residual interaction, Faessler *et al.*[53] have predicted asymmetries for higher 2^+ states in the Ni isotopes which bear little resemblance to the collective-model predictions. These predictions have not yet been tested by experiment.

[53] A. Faessler, N. K. Glendenning, and A. Plastino, Phys. Rev. 159, 846 (1967).

Figures 13 and 14 depict macroscopic model predictions for $l=3$ and $l=4$ transitions. Since the experimental curves of Fig. 5 show rather large variations from nucleus to nucleus, perhaps the qualitative agreement with the ^{56}Fe data shown in Fig. 13 is all that we should expect. Certainly the data are not sufficient to determine whether imaginary or spin-orbit distortions are necessary. The agreement with the 3^- differential cross section is good only at the forward peak. The collective model gives a poor account of the limited 4^+ asymmetry data. As shown in Fig. 14, the imaginary and spin-orbit interaction terms do not have a large effect, and they do not improve the fit to the ^{58}Ni data. If the 4^+ is assumed to be a two-phonon state in a strict vibrational model, the predictions are somewhat different but not in better agreement. In the first-order calculations, only multiple excitation via the first 2^+ state is allowed, while in second order, direct excitation of two phonons from the ground state is also permitted. While all these curves give poor fits to the ^{58}Ni data, the agreement with the 4^+ distribution of ^{54}Fe (Fig. 6) would clearly be much worse.

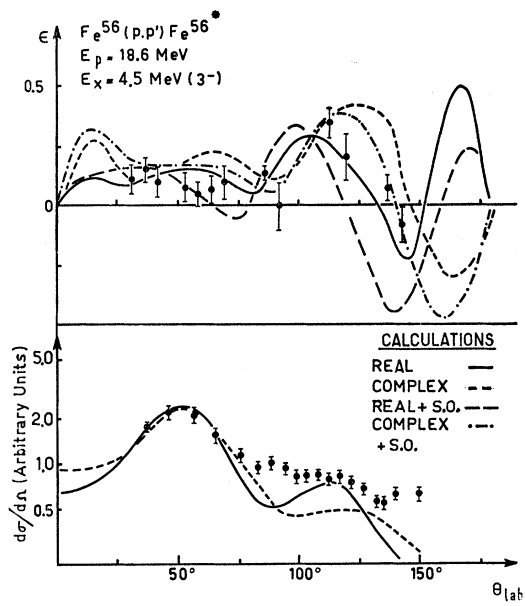

FIG. 13. Predictions of the asymmetry and cross section for the 3^- state in ^{56}Fe. Set-A optical and form-factor parameters were used.

V. CONCLUSION

In this initial survey, asymmetries have been measured for strongly excited states whose differential cross sections are well known. For the 2^+ states, these cross sections are generally regular but exhibit important differences, especially at back angles. The asymmetries measured for these states tend to fall into two groups distinguished by their magnitudes at 30° and 90°, but there is some evidence that this division is neater than the data warrant. The limited results for 3^- and 4^+ states shown here also reveal interesting variations.

The general features of the data for 2^+ states of the small group and for 3^- states can be predicted by the DWBA with a collective-model form factor. The effect of both imaginary and spin-orbit interaction terms in this model are smaller than at 40 MeV. While the distorted spin-orbit term at least generally improves the fit, the detailed variations produced by both these terms depend on the optical parameters. Unfortunately, the set of optical parameters which now gives the best fit to the inelastic asymmetry data does not give the best fit to the inelastic cross sections.

The collective model can not explain the large differences in the asymmetry for the two 2^+ states in ^{54}Fe. Only by artificially increasing the amplitude of the distorted spin-orbit term or by including an imaginary spin-orbut term in the optical potential were we able to fit even the magnitudes of the forward-angle asymmetry for the 1.41-MeV state. It is interesting to note that at 40 MeV the forward-angle region is the only place where the collective model encountered difficulties.

There is some promise that the more detailed microscopic model will be able to describe such data, since our phenomenological calculations indicated that the shape of the form factor does have an important effect on the asymmetry distribution. More realistic calculations for the higher 2^+ states in the Ni isotopes also predict large variations in shape. Such calculations indicate that it should be possible to derive nuclear-structure information directly from the asymmetry distributions. While the experimental curves for ^{54}Fe would tend to confirm this, the present microscopic predictions with a simple interaction do not fit the results. (It might also

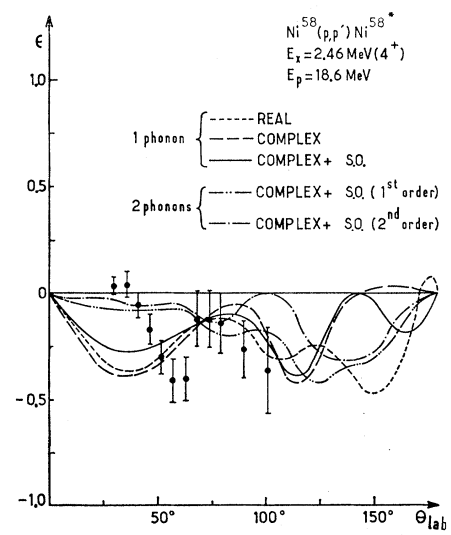

FIG. 14. Coupled-channels predictions of the asymmetry for the 4^+ state in ^{58}Ni. Set-A optical and form-factor parameters were used; β_4 was 0.2. A strict vibrational model was used for the 2-phonon calculations so that β_2 was 0.22 for both phonons, the same as β for the 1.45-MeV 2^+ state.

be expected that the $\frac{5}{2}^-$ and $\frac{7}{2}^-$ states in ^{63}Cu which apparently have quite different wave functions would also have different asymmetries. The fact that present measurements rule out large differences might be explained, however, on the basis that the single-particle contributions to these transitions are too small to affect the shape.)

Present indications are, then, that a more complex interaction is needed if the microscopic model is to work. While the addition of spin transfer did not affect the predictions very much, tensor interactions and the effects of antisymmetrization[54] should also be included in the calculations. Asymmetry data will provide a good test of such new calculations.

[54] K. A. Amos, V. A. Madsen, and I. E. McCarthy, Nucl. Phys. **A94**, 103 (1967).

ACKNOWLEDGMENTS

The authors gratefully acknowledge the indispensable help of R. Chaminade and the electronics group, Mrs. A. Garin and her co-workers in the detector laboratory, and of the entire cyclotron operating staff. A. Papineau kindly aided in several phases of the experimental work. We are indebted to Dr. J. Delaunay and Dr. P. Kossanyi-Demay for several calculations mentioned here, and to Dr. A. Forest for his microscopic-model form-factor program. We also thank Dr. M. Fricke, Dr. N. Glendenning, Dr. J. Lowe, Dr. F. G. Perey, Dr. G. R. Satchler, and Dr. A. Zucker for sending us unpublished reports of their work, as well as for several valuable discussions. The helpful comments of Dr. A. G. Blair, especially in the preparation of this paper, are greatly appreciated.

PHYSICAL REVIEW VOLUME 164, NUMBER 4 20 DECEMBER 1967

Study of Proton Particle-Hole States in ^{40}Ca by the ^{39}K(^{3}He,d)^{40}Ca Reaction*

KAMAL K. SETH
Northwestern University, Evanston, Illinois

AND

J. A. BIGGERSTAFF, P. D. MILLER, AND G. R. SATCHLER
Oak Ridge National Laboratory, Oak Ridge, Tennessee

(Received 7 July 1967)

Helium-3-induced charged-particle reactions on ^{39}K have been studied using a solid-state-detector dE/dx-E particle-identification telescope. Elastic-scattering angular distributions at ^{3}He energies of 12, 14, and 16 MeV as well as (^{3}He,d) angular distributions at 14 MeV have been measured. The reaction data are found to be characterized by extremely weak transitions to all known positive-parity excited states up to 5.3 MeV. Strong transitions to 15 negative-parity states up to 8.6-MeV excitation are observed and identified with the $T=0$ components of $(d_{3/2}^{-1}f_{7/2})$ and $(d_{3/2}^{-1}p_{3/2,1/2})$ configurations and the $T=1$ analogs of the ground-state quartet in ^{40}K having the $(d_{3/2}^{-1}f_{7/2})$ configuration. Since the distorted-wave method does not give a unique prescription for choosing between the various possible optical potentials which fit elastic scattering, a detailed examination is made of the effects of the choice specific ^{3}He and deuteron potentials, of the inclusion of spin-orbit coupling and nonlocality, and of the different approximations for the bound-state wave function; and the significance of the spectroscopic factors is discussed. The distorted-wave results are compared with the revised predictions of Gillet and Sanderson, and it is concluded that above and beyond the inherent uncertainties in the spectroscopic factors, Gillet and Sanderson's theoretical predictions agree poorly with the experimental results.

I. INTRODUCTION

IN the nuclear shell model ^{40}Ca, like ^{16}O, is of special importance because of its double-closed nature. In terms of the elementary shell model, the low-lying states of ^{40}Ca should have particularly simple particle configurations. The ground state should be doubly closed and spherical. The low-excitation negative-parity states should have 1-particle–1-hole configurations, with the particle being in the $f_{7/2}$, and $p_{3/2}$ (and to some extent $p_{1/2}$) orbitals and the hole being in the $d_{3/2}$ (and to some extent $s_{1/2}$ and $d_{5/2}$) orbitals. These negative-parity states should include two quartets of states with configurations $(d_{3/2}^{-1}f_{7/2})_{T=1}$ and $(d_{3/2}^{-1}p_{3/2})_{T=1}$. These are the analogs of the corresponding states[1] in ^{40}K and should start at approximately 7.6- and 9.6-MeV excitation, respectively, in ^{40}Ca. The positive-parity states are expected to be more complicated, involving excitations of $2p$-$2h$, $4p$-$4h$, etc., and having collective nature

* Research jointly sponsored by the U. S. Atomic Energy Commission under contract with Union Carbide Corporation and U. S. Army Research Office (Durham) under contract with Northwestern University.

[1] P. M. Endt and C. Van der Leun, Nucl. Phys. **34**, (1962).